Journal of Hydrology 501 (2013) 241–248

Contents lists available at ScienceDirect

Journal of Hydrology

journal homepage: www.elsevier.com/locate/jhydrol

How long does it take for aquifer recharge or aquifer discharge processes to reach steady state? ☆

Matthew J. Simpson [a,b,*], Farhad Jazaei [c], T. Prabhakar Clement [c]

[a] Mathematical Sciences, Queensland University of Technology, GPO Box 2434, Brisbane, Queensland 4001, Australia
[b] Tissue Repair and Regeneration Program, Institute of Health and Biomedical Innovation, Queensland University of Technology, Brisbane, Australia
[c] Department of Civil Engineering, Auburn University, Auburn, AL 36849, USA

ARTICLE INFO

Article history:
Received 17 April 2013
Received in revised form 4 July 2013
Accepted 5 August 2013
Available online 14 August 2013
This manuscript was handled by Peter K. Kitanidis, Editor-in-Chief, with the assistance of Ty Ferre, Associate Editor.

Keywords:
Aquifer recharge
Aquifer discharge
Mean action time
Variance of action time
Steady state
Time to steady state

SUMMARY

Groundwater flow models are usually characterized as being either transient flow models or steady state flow models. Given that steady state groundwater flow conditions arise as a long time asymptotic limit of a particular transient response, it is natural for us to seek a finite estimate of the amount of time required for a particular transient flow problem to effectively reach steady state. Here, we introduce the concept of *mean action time* (MAT) to address a fundamental question: how long does it take for a groundwater recharge process or discharge processes to effectively reach steady state? This concept relies on identifying a cumulative distribution function, $F(t;x)$, which varies from $F(0;x)=0$ to $F(t;x)\to 1^{-}$ as $t\to\infty$, thereby providing us with a measurement of the progress of the system towards steady state. The MAT corresponds to the mean of the associated probability density function $f(t;x)=\mathrm{d}F/\mathrm{d}t$, and we demonstrate that this framework provides useful analytical insight by explicitly showing how the MAT depends on the parameters in the model and the geometry of the problem. Additional theoretical results relating to the variance of $f(t;x)$, known as the *variance of action time* (VAT), are also presented. To test our theoretical predictions we include measurements from a laboratory-scale experiment describing flow through a homogeneous porous medium. The laboratory data confirms that the theoretical MAT predictions are in good agreement with measurements from the physical model.

1. Introduction

Groundwater flow systems, and the corresponding models used to study these systems, are typically characterized as being either transient or steady state (Remson et al., 1971; Bear, 1972; Clement et al., 1994; Haitjema, 1995; Strack, 1989; Wang and Anderson, 1982; Zheng and Bennett, 2002). This characterization is useful since the mathematical and computational techniques required to solve steady state groundwater flow models are generally much simpler than those required to solve transient groundwater flow models. Given that steady flow conditions correspond to the long time asymptotic limit of a transient response (Wang and Anderson, 1982, pp. 76–77; Haitjema, 1995, pp. 158–159) it is relevant to develop tools that can be used to estimate the amount of time required for a particular transient flow problem to effectively reach steady state. In the heat and mass transfer literature such a time is called a *critical time* (Hickson et al., 2009a,b, 2011).

A schematic diagram of a groundwater recharge problem is outlined in Fig. 1(a) for an aquifer of length L. The aquifer is bounded by two rivers. River one, at $x=0$, at river stage h_1, and river two, at $x=L$, at river stage h_2. The hypothetical phreatic surface without recharge is indicated by the curve marked $t=0$. We consider initiating a transient response in the groundwater flow system by applying spatially uniform recharge at rate R. The result of applying this recharge is that the amount of water stored in the aquifer increases with time as the phreatic surface rises to reach the curve indicated by $t\to\infty$. This kind of scenario, where recharge is applied to an existing unconfined groundwater flow system, leads to an increase in the saturated depth corresponding to an increase in the amount of water stored in the aquifer. The details of how to design and operate such recharge systems have been described at length previously (Bouwer, 2002; Daher et al., 2011; Martín-Rosales et al., 2007; Pedretti et al., 2012; Vandenbohede and Van Houtte, 2012). The design of such recharge systems naturally leads to the following questions:

* Corresponding author at: Mathematical Sciences, Queensland University of Technology, GPO Box 2434, Brisbane, Queensland 4001, Australia. Tel.: +61 7 3138 5241; fax: +61 7 3138 2310.
E-mail address: matthew.simpson@qut.edu.au (M.J. Simpson).

0022-1694/$ - see front matter © 2013 The Authors. Published by Elsevier B.V. All rights reserved.
http://dx.doi.org/10.1016/j.jhydrol.2013.08.005

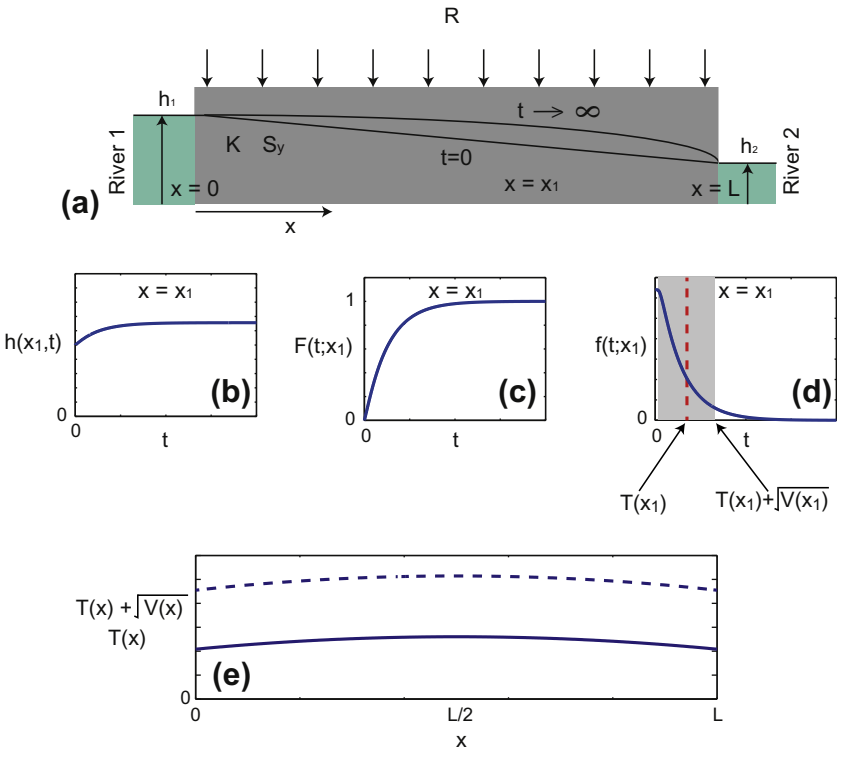

Fig. 1. (a) Schematic of an aquifer recharge process. The groundwater flow takes place on a one-dimensional domain, $0 \leqslant x \leqslant L$, and is assumed to correspond to a linearized, unconfined, Dupuit–Forchheimer description (Bear, 1972). The saturated depth at $x = 0$ (river 1) is $h(0,t) = h_1$. The saturated depth at $x = L$ (river 2) is $h(L,t) = h_2$. The schematic depicts a transition where the initial phreatic surface, indicated by $t = 0$, asymptotes to a new steady state, indicated by $t \to \infty$. This transition is associated with the application of uniform recharge, at rate R, for $t > 0$. (b) Schematic showing how the saturated thickness at a fixed location, $x = x_1$, in Fig. 1(a) varies with time, t. This schematic corresponds to a recharge transition since $h(x,t)$ increases with t. (c) For the schematic transition in (b) we show $F(t;x_1)$, which has the property that $F(0;x_1) = 0$ and $F(t;x_1) \to 1^-$ as $t \to \infty$. (d) For the schematic transition in (b) we plot $f(t;x_1)$, using Eq. (4). The mean of this probability density function is indicated in the red vertical (dotted) line, and corresponds to the MAT, $T(x_1)$. The variance of this probability density function is indicated with the gray shading, which corresponds to one standard deviation about the mean $T(x_1) \pm \sqrt{V(x_1)}$, as indicated. Profiles in (e) show $T(x)$ (solid) and $T(x) + \sqrt{V(x)}$ (dashed) at all locations $0 \leqslant x \leqslant L$. (For interpretation of the references to color in this figure legend, the reader is referred to the web version of this article.)

(1) How long does it take for the volume of water stored in the aquifer to reach a maximum? (i.e. what is the critical time for this process?)
(2) How does this critical time depend on the parameters governing the flow processes and the geometry of the aquifer?

Strictly speaking, from a mathematical point of view, it takes an infinite amount of time for a transient response of a diffusive process to become steady (McNabb and Wake, 1991; McNabb, 1993). Clearly, this strict mathematical definition is impractical and it would be useful to have a quantitative framework to estimate a finite timescale that indicates when the time rate of change of water stored in the aquifer to effectively reach zero (Sophocleus, 2012; Walton, 2011). Developing a method of analysis that avoids the need for relying on numerical computation to answer these questions would be useful since it is not obvious how, for example, changing the properties of the porous medium or the geometry of the groundwater flow system would affect the time taken for the rate of change of water stored in the aquifer to effectively reach zero. Understanding this timescale may have several practical uses; for example, if we were to design an artificial recharge program it would be of interest to monitor the increase in storage in the aquifer with time and to have a criteria to indicate when the system would effectively reach steady state.

Previous attempts to characterize critical times for groundwater flow models have relied on using numerical experimentation (Buès and Oltean, 2000; Chang et al., 2011), laboratory-scale experimentation (Kim and Ann, 2001; Goswami and Clement, 2007; Chang and Clement, 2012; Simpson et al., 2003) or very simple mathematical definitions. One common mathematical approach is to define the critical time to be the amount of time taken for the transient solution to reach within ϵ% of the corresponding steady state value, where ϵ is some small user-defined tolerance (Hickson et al., 2011; Landman and McGuinness, 2000; Lu and Werner, 2013; Watson et al., 2010). Although insightful, there are certain difficulties associated with this definition, namely:

(1) this definition depends upon a subjective choice of ϵ,
(2) this definition requires the complete solution of the the transient groundwater flow problem, and
(3) this definition leads to a numerical framework that does not provide analytical insight into how the critical time varies with the parameters in the model.

In this work we introduce the concept of *mean action time* (MAT) which gives us a finite estimate of the amount of time required for a transient groundwater flow resposne to effectively reach steady state. The MAT was originally defined by McNabb and Wake as a tool to study linear heat transfer (McNabb and Wake, 1991; McNabb, 1993). Here we demonstrate how to extend this theory to analyze groundwater flow processes. We will show, in a general framework, that:

(1) the MAT gives us an objective finite estimate of the amount of time required for a transient response to effectively reach steady state,

(2) the MAT can be found explicitly without solving the governing transient groundwater flow equation, and
(3) the mathematical expression for the MAT shows us how the timescale for different transitions, such as applying or removing different amounts of recharge, would depend on the parameters in the groundwater flow model.

Furthermore, once we have defined the MAT, we can also define higher moments such as the variance of action time (VAT) which provides a measure of the spread of the distribution about the mean (Ellery et al., 2012b, 2013; Simpson et al., 2013). The VAT is useful since we know that if the VAT is small then we are dealing with a low-variance distribution for which the mean value provides a useful estimate of the timescale of interest (Ellery et al., 2012b; Grimmett and Welsh, 1986). Alternatively, if the VAT is large then we are dealing with a high-variance distribution for which the mean value is less insightful (Ellery et al., 2012b; Grimmett and Welsh, 1986). For such high variance distributions we can improve our estimate of the time required for the system to reach steady state by incorporating information about the variance (Simpson et al., 2013), as we shall demonstrate in Section 3.

In this work we aim to first present the mathematical derivations and assumptions in a general framework. Once we have developed the theoretical results we then apply these concepts to obtain specific MAT and VAT results for a new laboratory-scale experimental data set describing aquifer recharge and discharge processes.

2. Theoretical methods

We consider a one-dimensional, unconfined, Dupuit–Forchheimer model of groundwater flow through a saturated homogeneous porous medium (Bear, 1972, 1979)

$$S_y\frac{\partial h}{\partial t}=K\frac{\partial}{\partial x}\left[h\frac{\partial h}{\partial x}\right]+R, \tag{1}$$

where $h(x,t)>0$ [L] is the saturated thickness at position x and time t, $S_y>0$ [–] is the specific yield, $K>0$ [L/T] is the saturated hydraulic conductivity and $R>0$ [L/T] is the recharge rate. For practical problems where the hydraulic gradient is very small, $|\partial h/\partial x|\ll 1$, this model is often linearized to give

$$S_y\frac{\partial h}{\partial t}=K\bar{h}\frac{\partial^2 h}{\partial x^2}+R, \tag{2}$$

where $\bar{h}$ is the average saturated thickness (Bear, 1972, 1979; Haitjema, 1995; Strack, 1989). This simplification is sufficiently robust for treating many problems (Haitjema, 1995; Strack, 1989) including certain laboratory-scale systems (Kim and Ann, 2001). For notational convenience we will re-write Eq. (2) in the form of a reaction–diffusion equation

$$\frac{\partial h}{\partial t}=D\frac{\partial^2 h}{\partial x^2}+W, \tag{3}$$

where $D=K\bar{h}/S_y$ [L^2/T] is the diffusivity and $W=R/S_y$ [L/T] is a zero order constant source term which is used to model recharge (Bear, 1979).

To apply our modeling framework to the schematic in Fig. 1(a), we will consider a model of unconfined groundwater flow, Eq. (3), that describes an arbitrary transition from some initial condition, $h(x,0)=h_0(x)$, to some steady state $\lim_{t\to\infty}h(x,t)=h_\infty(x)$. This transition is sufficiently general that it could describe an aquifer recharge process, where $h_\infty(x)\geqslant h_0(x)$ for all locations x, such as the case where additional recharge applied by increasing R. Similarly, our framework could describe an aquifer discharge process, where $h_\infty(x)\leqslant h_0(x)$ for all locations x, such as the case where the recharge applied to the system is reduced, by decreasing R. We seek to characterize the amount of time required for such transitions to effectively reach steady state by considering the following quantities (Ellery et al., 2012a,b):

$$F(t;x)=1-\left[\frac{h(x,t)-h_\infty(x)}{h_0(x)-h_\infty(x)}\right],\quad t>0,$$
$$f(t;x)=\frac{\mathrm{d}F(t;x)}{\mathrm{d}t}=-\frac{\partial}{\partial t}\left[\frac{h(x,t)-h_\infty(x)}{h_0(x)-h_\infty(x)}\right],\quad t>0. \tag{4}$$

For many transitions $F(t;x)$ monotonically increases from $F=0$ at $t=0$ to $F\to 1^-$, as $t\to\infty$ at all spatial locations x, as shown in Fig. 1(b)–(c). Here, $F(t;x)$ and $f(t;x)$ as functions of time t, at a particular location x, which can be thought of as a parameter. The properties of these functions mean that we can interpret $F(t;x)$ as a cumulative distribution function and $f(t;x)$ as the associated probability density function (Ellery et al., 2012a,b). From a physical point of view, our interpretation of these definitions is as follows: at $t=0$, we have $F=0$, meaning that 0% of transient response has taken place. In the long time limit as $t\to\infty$, we have $F=1$, meaning that 100% of the transient response has occurred. For intermediate values of t we have $0<F<1$, meaning that $(100\times F)$% of the transient response has occurred. For example, if $F(t;x)=1/2$, then we can interpret this as 50% of the transient response has taken place by this time.

The MAT, $T(x)$, is the mean of this distribution which has the probability density function $f(t;x)$, and can be written as (Ellery et al., 2012b)

$$T(x)=\int_0^\infty tf(t;x)\,\mathrm{d}t. \tag{5}$$

Physically, we interpret the MAT to be the mean timescale required for the initial condition, $h_0(x)$, to asymptote to the steady state, $h_\infty(x)$. Intuitively, we expect that this timescale would depend on spatial location and we will see that the MAT is indeed a function of position, x. To evaluate the MAT we apply integration by parts to Eq. (5) to obtain

$$T(x)g(x)=\int_0^\infty h_\infty(x)-h(x,t)\,\mathrm{d}t, \tag{6}$$

where we have defined $g(x)=h_\infty(x)-h_0(x)$ for notational convenience. To arrive at Eq. (6) we made use of the fact that $h(x,t)-h_\infty(x)$ decays to zero exponentially fast as $t\to\infty$, which is true for all linear reaction diffusion equations (Ellery et al., 2012a,b). Differentiating Eq. (6) twice with respect to x and combining the resulting expression with Eq. (3), gives us

$$\frac{\mathrm{d}^2[T(x)g(x)]}{\mathrm{d}x^2}=-\frac{g(x)}{D}, \tag{7}$$

or, if we expand using the product rule, we can write this as

$$\frac{\mathrm{d}^2T(x)}{\mathrm{d}x^2}+\frac{\mathrm{d}T(x)}{\mathrm{d}x}\left[\frac{2}{g(x)}\frac{\mathrm{d}g(x)}{\mathrm{d}x}\right]+T(x)\left[\frac{1}{g(x)}\frac{\mathrm{d}^2g(x)}{\mathrm{d}x^2}\right]=-\frac{1}{D}, \tag{8}$$

which is a boundary value problem for the MAT, $T(x)$. We would like to emphasize that Eq. (8) is sufficiently general that it applies to any initial condition, $h_0(x)$, and any steady state, $h_\infty(x)$, such that $F(t;x)$ monotonically increases from $F=0$ at $t=0$ to $F\to 1^-$ as $t\to\infty$ for all x. This means that Eq. (8) can be used to characterize the amount of time required for a transition to reach steady state for a very general class of aquifer recharge and discharge processes. Furthermore the approach is valid for any values of S_y, K, R, L, h_1 and h_2. We note that our derivation of Eq. (8) is very similar to previous work presented by Ellery and coworkers (Ellery et al., 2012a,b) except that those previous studies considered a first order linear source term in the governing equations whereas here we consider a zero order constant source term.

The theory of MAT relies on certain properties of the problem that guarantee that the improper integral for $T(x)$, given by Eq. (5), is convergent. When we apply the definition of MAT in the present context we are guaranteed that the improper integral in Eq. (5) is convergent since $h(x,t) - h_\infty(x)$ decays to zero exponentially fast as $t \to \infty$ for all such reaction diffusion equations (Ellery et al., 2012a,b; Hickson et al., 2011). Alternative definitions of a critical time, such as considering the median of action time, where $F(t;x) = 1/2$, do not allow us to make use of this asymptotic property and consequently we cannot solve for the critical time without having previously solved the underlying partial differential equation governing for the transient solution, $h(x,t)$.

Similar to how we calculated the mean of $f(t;x)$, we can also evaluate higher moments of $f(t;x)$, such as the variance, which quantifies the spread about the mean (Ellery et al., 2012b, 2013; Simpson et al., 2012). We begin by using the standard definition of the variance

$$V(x) = \int_0^\infty (t - T(x))^2 f(t;x)\,\mathrm{d}t. \tag{9}$$

Expanding the quadratic term in the integrand in Eq. (9) allows us to evaluate two of the three integral expressions on the right hand side of Eq. (9) in terms of the MAT, $T(x)$. The remaining integral can be simplified using integration by parts, making use of the fact that $h(x,t) - h_\infty(x)$ decays to zero exponentially fast as $t \to \infty$ to give

$$\psi(x) = 2\int_0^\infty t(h_\infty(x) - h(x,t))\,\mathrm{d}t, \tag{10}$$

where we have made a change of variables, $\psi(x) = V(x)g(x) + T(x)^2 g(x)$, to simplify the expression. To obtain a differential equation for $\psi(x)$ we differentiate Eq. (10) twice with respect to x. Combining the resulting expression with Eq. (3) gives us

$$\frac{\mathrm{d}^2\psi(x)}{\mathrm{d}x^2} = -\frac{2T(x)g(x)}{D}, \tag{11}$$

which, together with appropriate boundary conditions can be solved for $\psi(x)$ and in turn rearranged to give $V(x)$, recalling that $V(x) = \psi(x)/g(x) - T(x)^2$. Once we have solved the relevant boundary value problems for $T(x)$ and $V(x)$, we can identify a time interval $t \in [T(x) - \sqrt{V(x)}, T(x) + \sqrt{V(x)}]$. Here, we take the time interval to be the mean plus or minus one standard deviation of the distribution $f(t;x)$ (Simpson et al., 2013). Once we have calculated the mean and variance of $f(t;x)$ at a particular location, as indicated in Fig. 1(d), we can put this information together to view how the MAT and VAT varies with position, as indicated in Fig. 1(e).

To reiterate the practicality of our results, we would like to emphasize the following points. From a strict mathematical point of view, the transient solution of a reaction diffusion equation, such as Eq. (3), takes an infinite amount of time to reach steady state (McNabb and Wake, 1991; McNabb, 1993). Using this strict definition, it is completely unclear how to make a practical estimate of the duration of time that a transient groundwater process will require to reach steady state. Instead we use the MAT as a finite estimate of the amount of time required for the transient flow process to effectively reach steady state.

2.1. MAT and VAT for aquifer recharge

Although we have outlined the MAT theory in Section 2 for an arbitrary aquifer recharge or discharge process, we will now demonstrate the insight provided by the MAT framework by considering a specific application. We will examine the transition described by Eq. (3) on $0 \leqslant x \leqslant L$ with boundary conditions $h(0,t) = h_1$ and $h(L,t) = h_2$. We consider a transition from the initial condition,

$$h_0(x) = \frac{x(h_2 - h_1)}{L} + h_1, \tag{12}$$

to a new steady state that is driven by applying recharge, R, for $t > 0$. The long time steady state for this transition is

$$\lim_{t\to\infty} h(x,t) = h_\infty(x) = -\frac{Wx^2}{2D} + x\left[\frac{h_2 - h_1}{L} + \frac{WL}{2D}\right] + h_1, \tag{13}$$

where $D = K\bar{h}/S_y$ and $W = R/S_y$. This particular initial condition and steady state gives us

$$g(x) = \frac{Wx(L-x)}{2D}. \tag{14}$$

To find the MAT for this transition we note that $\mathrm{d}g(x)/\mathrm{d}x = W(L-2x)/(2D)$ and $\mathrm{d}^2g(x)/\mathrm{d}x^2 = -W/D$. Substituting these expressions for $g(x)$, $\mathrm{d}g(x)/\mathrm{d}x$ and $\mathrm{d}^2g(x)/\mathrm{d}x^2$ into Eq. (8) gives

$$\frac{\mathrm{d}^2T(x)}{\mathrm{d}x^2} + \frac{\mathrm{d}T(x)}{\mathrm{d}x}\left[\frac{2(L-2x)}{x(L-x)}\right] + T(x)\left[\frac{-2}{x(L-x)}\right] = -\frac{1}{D}, \tag{15}$$

which is a variable coefficient second order boundary value problem that is singular at $x = 0$ and $x = L$. We note that Eq. (15) is independent of W, and this can be explained by the fact that the coefficients of $\mathrm{d}T(x)/\mathrm{d}x$ and $T(x)$ in Eq. (8) are rational functions in which W cancels for our $g(x)$, given by Eq. (14).

To determine the relevant boundary conditions for Eq. (15) we multiply both sides of this equation by $x(L-x)$, which gives

$$x(L-x)\frac{\mathrm{d}^2T(x)}{\mathrm{d}x^2} + 2(L-2x)\frac{\mathrm{d}T(x)}{\mathrm{d}x} - 2T(x) = -\frac{x(L-x)}{D}. \tag{16}$$

Evaluating Eq. (16) at $x = 0$ gives us

$$\frac{\mathrm{d}T(0)}{\mathrm{d}x} - \frac{T(0)}{L} = 0, \tag{17}$$

which is a Robin condition for the boundary at $x = 0$ (Kreyszig, 2006; Zill and Cullen, 1992). To determine the other boundary condition we substitute $x = L$ into Eq. (16) to give

$$\frac{\mathrm{d}T(L)}{\mathrm{d}x} - \frac{T(L)}{L} = 0, \tag{18}$$

which is a Robin condition at $x = L$ (Kreyszig, 2006; Zill and Cullen, 1992).

The solution of Eq. (15) with Eqs. (17) and (18) is

$$T(x) = \frac{1}{12D}(L^2 + xL - x^2). \tag{19}$$

This solution shows that the MAT is spatially dependent and has a maximum value of $5L^2/(48D)$ at $x = L/2$. This expression is very revealing since it shows us exactly how the MAT depends on the parameters in the model and the boundary conditions. We see that the MAT depends on the ratio L^2/D, which is a diffusive timescale (Barenblatt, 2003).

Now that we have solved for the MAT we can use Eq. (11), with the relevant boundary conditions $\psi(0) = \psi(L) = 0$, to solve for $\psi(x)$ which can be rearranged to give

$$V(x) = \frac{1}{720D^2}\left(7L^4 + 2L^3x - 3L^2x^2 + 2x^3L - x^4\right). \tag{20}$$

The maximum VAT occurs at $x = L/2$ and is given by $119L^4/(11520D^2)$. The expression for the maximum variance can be used to find the maximum standard deviation, which is given by $\sqrt{119}L^2/(\sqrt{11520}D) \approx 0.1016L^2/D$.

2.2. MAT and VAT for aquifer discharge

We now consider a transition governed by Eq. (3) for the process of aquifer discharge. With the same domain and boundary

conditions described for the recharge problem in Section 2.1, we consider the initial condition

$$h_0(x) = -\frac{Wx^2}{2D} + x\left[\frac{h_2 - h_1}{L} + \frac{WL}{2D}\right] + h_1, \tag{21}$$

which corresponds to the long term steady state profile from the recharge process described in Section 2.1, where $D = K\bar{h}/S_y$ and $W = R/S_y$. To initiate a discharge process, where the saturated thickness of the aquifer will decrease with time, we set $R = 0$ in Eq. (2), which is equivalent to setting $W = 0$ in Eq. (3), which gives

$$\lim_{t\to\infty} h(x,t) = h_\infty(x) = \frac{x(h_2 - h_1)}{L} + h_1, \tag{22}$$

and

$$g(x) = -\frac{Wx(L-x)}{2D}. \tag{23}$$

With these conditions, Eq. (8) can be written as

$$\frac{d^2T(x)}{dx^2} + \frac{dT(x)}{dx}\left[\frac{2(L-2x)}{x(L-x)}\right] + T(x)\left[\frac{-2}{x(L-x)}\right] = -\frac{1}{D}, \tag{24}$$

which is exactly the same boundary value problem as we obtained previously in Section 2.1. The fact that the boundary value problem governing the MAT for the discharge process is exactly the same as the boundary value problem governing the MAT for the recharge process means that the exact same Robin boundary conditions and the exact same solution, namely Eq. (19), are relevant for both the recharge and discharge problems. Similarly, we can also solve Eq. (11) to find the VAT for this discharge problem. Following the same procedure to evaluate the VAT, we find that the solution of Eq. (11) for the discharge problem is exactly the same as for the recharge problem, namely Eq. (20). This result shows that the MAT and VAT for the aquifer recharge and discharge processes are identical.

3. Results

We now demonstrate the practicality of our theoretical predictions from Sections 2.1 and 2.2 by considering new datasets derived from aquifer recharge and discharge experiments completed in our laboratory. We performed experiments in a laboratory-scale aquifer model, packed with a homogeneous porous medium, by applying different amounts of recharge to the system and measuring the temporal response of the saturated depth in the system. Our experimental data will give us an indication of the amount of time required for the saturated thickness of the laboratory-scale aquifer to reach steady state and we will test these measurements against predictions made according to the MAT and VAT results developed in Section 2. We will test the MAT and VAT theory for both aquifer recharge and aquifer discharge experiments.

3.1. Case study: analysis of a new laboratory-scale data set

A laboratory-scale aquifer model, similar to the one used in several previous studies (Goswami and Clement, 2007; Abarca and Clement, 2009; Chang and Clement, 2012, 2013) was used, and an image of the physical model is shown in Fig. 2(a). The tank was constructed of Pexiglass. The central porous chamber (50 cm × 28 cm × 2.2 cm) was packed under wet conditions with uniformly-sized glass beads, where each bead has a diameter of 1.1 mm. We consider the glass bead system to be a homogeneous and isotropic porous medium (Goswami and Clement, 2007; Abarca and Clement, 2009; Chang and Clement, 2012, 2013). A constant head boundary condition was applied at the left-hand vertical boundary, where $x = 0$ cm, to maintain an initial saturated depth of approximately *18.7* cm. A no-flow boundary was imposed at the right-hand vertical boundary, where $x = 50$ cm.

A recharge gallery, consisting of approximately evenly spaced constant flow drippers, was installed along the upper boundary of the tank. Water was delivered to the recharge outlets from a constant head tank. We considered two different kinds of experiments and repeated each experiment for three different recharge rates:

(1) For the *recharge experiments*, we considered the initial condition in the system to be at a spatially uniform saturated depth $h_0(x) = h_1 \approx 18.7$ cm. At $t = 0$ the recharge was applied and the increase in saturated thickness at the right hand boundary, where $x = 50$ cm, was recorded using the scale shown in Fig. 2(b). The recharge experiments were repeated three times using three different recharge rates: $R_1 = 1.23$ cm/min, $R_2 = 1.77$ cm/min, and $R_3 = 2.57$ cm/min.
(2) The *discharge experiments* were initiated by removing the recharge gallery at the conclusion of each recharge experiment. This means that after a sufficient period of time (approximately 5 min), at the conclusion of each recharge experiment, the phreatic surface was approximately parabolic and each discharge experiment involved observing the parabolic phreatic surface relaxing back to an essentially horizontal phreatic surface.

The recharge rates used in the experiments are relatively large, and the reason that we used such large recharge rates was so that we could make our measurements as accurate as possible. For the recharge experiments, we expect that initial saturated depth, $h_0(x)$, will increase to $h_\infty(x)$ after a sufficient amount of time. Since we are aiming to make accurate measurements of the increase in $h(x,t)$, it is convenient for us to use relatively large recharge rates to ensure that the difference between $h_\infty(x)$ and $h_0(x)$ was approximately 2–3 cm so that we could record these measurements as accurately as possible using the scale shown in Fig. 2(b).

We first report results for the recharge experiments. Results in Fig. 3(a)–(c) show the transient response at $x = 50$ cm in the laboratory-scale aquifer when applying three different recharge rates: $R_1 = 1.23$ cm/min, $R_2 = 1.77$ cm/min and $R_3 = 2.57$ cm/min, respectively. Comparing the profiles in Fig. 3(a)–(c) indicates that each of the recharge experiments were initiated with $h(50,0) \approx 18.7$ cm, and we observe that the increase in saturated thickness at $x = 50$ cm depends on the recharge rate. For example, with $R_1 = 1.23$ cm/min we see that $h(50,t)$ eventually increases to approximately 19.9 cm, for $R_2 = 1.77$ cm/min we see that $h(50,t)$ eventually increases to approximately 20.5 cm and for $R_3 = 2.57$ cm/min $h(50,t)$ eventually increases to approximately 22.3 cm. Interestingly, a visual comparison of the three transient data sets in Fig. 3(a)–(c) indicates that it is very difficult to distinguish the differences in the timescales of the transient processes regardless of the differences in the recharge rate and the differences in the change in saturated thickness at $x = 50$ cm. This qualitative observation is consistent with our theoretical predictions from Section 2.1 where the MAT framework predicted that the recharge timescale is independent of the recharge rate. We will now quantitatively test this prediction using the data from Fig. 3(a)–(c).

To compute the values of $f(t;x)$ we used the data from Fig. 3(a)–(c), at $x = 50$ cm, and estimated $h_0(x)$ and $h_\infty(x)$ directly from these data. To reconstruct $f(t;x)$ for this data we rewrite Eq. (4) as

$$f(t;x) = \frac{1}{h_\infty(x) - h_0(x)}\frac{\partial h(x,t)}{\partial t} \approx \frac{1}{h_\infty(x) - h_0(x)}\left[\frac{h(x,t+\delta t) - h(x,t-\delta t)}{2\delta t}\right], \tag{25}$$

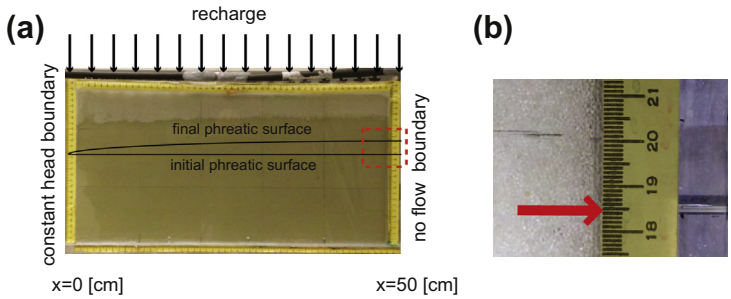

Fig. 2. (a) Laboratory-scale apparatus. The porous media chamber was wet-packed with uniform glass beads. A constant head boundary was imposed at $x = 0$ cm and a no flow boundary was imposed at $x = 50$ cm. The initial condition corresponds to an approximately horizontal phreatic surface, as indicated. The recharge was applied approximately uniformly along the top of the porous media chamber and eventually the phreatic surface evolves to the final state, as indicated. Observations were made by monitoring the saturated depth of the fluid at $x = 50$ cm. The region contained within the (red) dashed square in (a) is shown in (b) where the saturated thickness is indicated by the red arrow. (For interpretation of the references to color in this figure legend, the reader is referred to the web version of this article.)

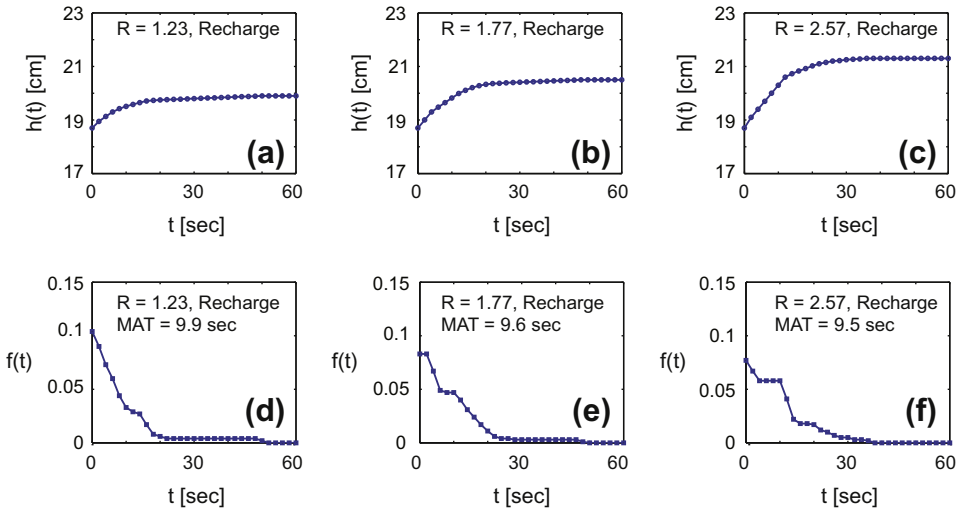

Fig. 3. Results for the recharge experiments are given in (a)–(c) showing the evolution of $h(x,t)$, at $x = 50$ cm, for $R_1 = 1.23$ cm/min, $R_2 = 1.77$ cm/min and $R_3 = 2.57$ cm/min, respectively. Using the data in (a)–(c), collected at 2 s intervals, profiles of $f(t;x)$ at $x = 50$ cm were estimated using Eq. (25), and presented in (d)–(f). Estimates of the MAT at $x = 50$ cm were obtained by numerically integrating Eq. (5) and the results are reported in (d)–(f).

where we have used a central difference approximation to estimate $\partial h/\partial t$ (Chapra and Canale, 2009). This discrete expression for $f(t;x)$ can be evaluated using the $h(x,t)$ time series data presented in Fig. 3(a)–(c). The corresponding $f(t;x)$ profiles, at $x = 50$ cm, shown in Fig. 3(d)–(f), are given for the three different recharge rates: $R_1 = 1.23$ cm/min, $R_2 = 1.77$ cm/min and $R_3 = 2.57$ cm/min, respectively. To quantitatively test our theoretical predictions from Section 2.1 we evaluate $T(x)$, at $x = 50$ cm, using Eq. (5) and the $f(t;x)$ data in Fig. 3(d)–(f). The integral expression is evaluated numerically using a trapezoid rule with panel width of 2 s (Chapra and Canale, 2009). The corresponding values of the MAT, estimated directly from the data, are 9.9, 9.6 and 9.5 s for each of the three recharge experiments, respectively. These results indicate that the MAT for the experiments appear to be independent of the recharge rate, as predicted by our theory in Section 2.1.

We now report the results of the discharge experiments. Results in Fig. 4(a)–(c) show the transient response at $x = 50$ cm in the laboratory-scale aquifer after turning off the recharge at the conclusion of each of the three recharge experiments where different rates of recharge had been applied: $R_1 = 1.23$ cm/min, $R_2 = 1.77$ cm/min and $R_3 = 2.57$ cm/min. Comparing the profiles in Fig. 4(a)–(c) confirms that each of the discharge experiments were initiated with different values of the saturated thickness at $x = 50$ cm. However, the data in Fig. 4(a)–(c) indicates that after a sufficiently long period of time the saturated thickness at $x = 50$ cm asymptotes to approximately 18.7 cm. A visual comparison of the three transient discharge data sets in Fig. 4(a)–(c) indicates that the timescale of the transient processes are very similar regardless of the initial saturated depth at $x = 50$ cm. This qualitative observation is consistent with our theoretical predictions from Sections 2.1 and 2.2 and we will now quantitatively test this prediction using the data from Fig. 4(a)–(c).

The profiles in Fig. 4(d)–(f) show $f(t;x)$ at $x = 50$ cm, for each discharge experiment. To compute the values of $f(t;x)$ we used Eq. (25) with the data from Fig. 4(a)–(c). For each discharge experiment we estimate $T(x)$, using Eq. (5) and our $f(t;x)$ data in Fig. 4(d)–(f). To evaluate the integral in Eq. (5) we use the trapezoid rule with panel width of 2 s (Chapra and Canale, 2009). The corresponding values of the MAT, estimated directly from the data, are 9.5, 9.7 and 10.4 s for each of the three discharge experiments. These results are also consistent with our MAT predictions since our theoretical results in Sections 2.1 and 2.2 predicted that the mean timescale for the discharge process is identical to the mean timescale for the recharge process.

Our laboratory data, described so far, qualitatively supports the theoretical predictions made using the MAT framework in Sections 2.1 and 2.2. To quantitatively test our theoretical predictions we must estimate the parameters describing the fluid flow in the laboratory scale model. We measured the saturated hydraulic conductivity using a standard column test which showed that the average

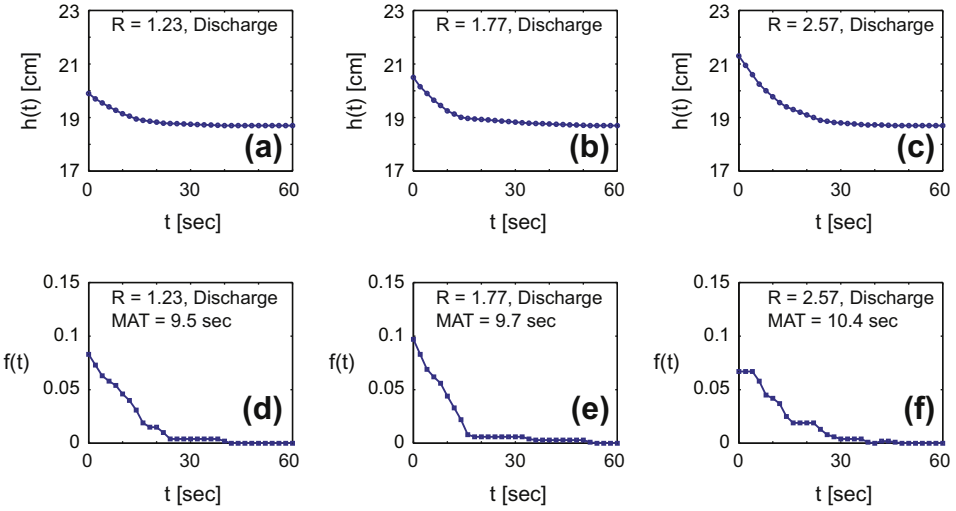

Fig. 4. Results for the discharge experiments are given in (a)–(c) showing the evolution of $h(x,t)$, at $x = 50$ cm, for $R_1 = 1.23$ cm/min, $R_2 = 1.77$ cm/min and $R_3 = 2.57$ cm/min, respectively. Using the data in (a)–(c), collected at 2 s intervals, profiles of $f(t;x)$ at $x = 50$ cm were estimated using Eq. (25), and presented in (d)–(f). Estimates of the MAT at $x = 50$ cm were obtained by numerically integrating Eq. (5) and the results are reported in (d)–(f).

saturated hydraulic conductivity is 980 m/day (68 cm/min). We independently measured the specific yield, $S_y \approx 0.2$, and we estimated that the average saturated depth was $\bar{h} \approx 19.0$ cm so that we can estimate $D = K\bar{h}/S_y$ to be 6460 cm^2/min. This gives a maximum MAT, $5L^2/(48D)$, of 9.7 s. Here we have used $L = 100$ cm to reflect the symmetry of the problem imposed by using a no flow boundary condition at $x = 50$ cm. This theoretical prediction agrees with our experimental measurements reported in Figs. 3 and 4.

If we wish to use our MAT and VAT results to quantitate a critical time interval for the experimental data we take the critical time interval to be the mean plus or minus one standard deviation (Simpson et al., 2013). Using $K = 980$ m/day, $S_y = 0.2$ and $\bar{h} = 19.0$ cm indicates that the maximum VAT is approximately 89.0 s^2 for all our experimental systems. This means that we can take the critical time interval to be $9.7 \pm \sqrt{89} \approx 9.7 \pm 9.4$ s, which indicates that by 19.1 s the transient aquifer response has essentially finished. Comparing this estimate with the data in Figs. 3, 4 and Fig. 4(a)–(c) seems reasonable since we observe little transient response in the system after approximately 20 s for each experimental dataset.

4. Discussion and conclusions

The theory of MAT provides us with an objective tool to characterize the timescale required for a transient groundwater flow response to effectively reach steady state. This is a practical tool since it allows us to estimate the timescale required for a transient response to effectively reach steady state using an exact analytical framework that avoids the need for solving a time dependent partial differential equation describing the transient process.

The key advantage of our approach is that we arrive at exact mathematical expressions for the MAT and VAT and we can see exactly how these quantities depend on the parameters (e.g. $K, \bar{h}, S_y, h_1, h_2, L$ and R) for a general aquifer recharge and aquifer discharge processes. Our theoretical results yield some useful and possibly counterintuitive results. For example, we show that the MAT is not explicitly dependent upon the recharge rate, R, and we show that the MAT for a recharge process is equivalent to the MAT of the related discharge process. This is a surprising result since the steady state phreatic surface depends on the recharge rate R but the new theory indicates that the time taken to reach steady state is independent of R. These results are not obvious without the MAT framework.

In addition to providing more general insight into aquifer recharge and discharge processes, we also evaluated the MAT for a specific laboratory-scale data set describing unconfined aquifer recharge and discharge processes. The theory predicted that the MAT for the three recharge and the three discharge experiments should be 9.7 s. Despite experimental variabilities, all six MAT values (9.9, 9.6 and 9.5 s for recharge; and 9.5, 9.7, and 10.4 s for discharge) estimated from transient dataset are remarkably close the theoretical prediction, demonstrating the validity of the theory.

The MAT analysis and results outlined here can be applied to study other linear models of groundwater flow, such as two-dimensional and three-dimensional models (Landman and McGuinness, 2000). For such models, the techniques outlined here for the one-dimensional case are directly applicable except that the boundary value problems governing the MAT will be two-dimensional and three-dimensional partial differential equations, similar to Poisson's equation (Wang and Anderson, 1982). These kinds of equations can be solved exactly using standard techniques, such as separation of variables, provided that the problems are considered on separable domains (Kreyszig, 2006). Other problems, such as studying the MAT of genuinely nonlinear flow problems that are not readily linearized are far more challenging (Ellery et al., 2012a; Simpson et al., 2013). The application of the theory of MAT to such problems requires additional analysis and our future work will seek to address these problems.

An extension of our present study would be to consider the MAT for a heterogeneous groundwater flow problem. The heterogeneous analog of Eq. (1) can be written as

$$S_y \frac{\partial h}{\partial t} = \frac{\partial}{\partial x}\left[K(x)h\frac{\partial h}{\partial x}\right] + R(x), \tag{26}$$

where $K(x)$ is the spatially varying saturated hydraulic conductivity and $R(x)$ is the spatially varying recharge rate (Bear, 1979). For practical problems where the hydraulic gradient is very small, $|\partial h/\partial x \ll 1|$, the linearized analog of this model can be written as

$$\frac{\partial h}{\partial t} = \frac{\partial}{\partial x}\left[D(x)\frac{\partial h}{\partial x}\right] + W(x), \tag{27}$$

where $D(x) = \bar{h}K(x)/S_y$ [L^2/T] is a spatially-dependent diffusivity and $W(x) = R(x)/S_y$ is a spatially dependent zero order source term.

If we apply the same mathematical procedure, outlined previously in Section 2, to find the boundary value problem governing the MAT for the heterogeneous flow model we arrive at

$$\frac{d^2[T(x)g(x)]}{dx^2} + \frac{1}{D(x)}\frac{dD(x)}{dx}\frac{d[T(x)g(x)]}{dx} = -\frac{g(x)}{D(x)}, \tag{28}$$

which is a generalization of Eq. (7) since the two boundary value problems are identical when $D(x)$, or equivalently $K(x)$, is a constant. Similar to the homogeneous flow problem, the MAT for the heterogeneous flow problem is independent of the recharge, but is now explicitly dependent on the form of the heterogeneity since the solution of Eq. (28) depends on the functional form of $D(x)$. Although we have outlined how the theory of MAT extends to deal with the heterogeneous flow, we leave a thorough exploration of the solution of Eq. (28) and a comparison of such a solution with physical measurements as a topic for future research.

Acknowledgements

We appreciate support from Queensland University of Technology, Auburn University and the Australian Research Council Discovery Project Grant DP120100551. This work was, in part, supported by the National Science Foundation Grant NSF-EAR-0943679B.

References

Abarca, E., Clement, T.P., 2009. A novel approach for characterizing the mixing zone of a saltwater wedge. Geophysical Research Letters 36, L06402.
Barenblatt, G.I., 2003. Scaling. Cambridge University Press, Cambridge, UK.
Bear, J., 1972. Dynamics of Fluids in Porous Media. Springer, New York.
Bear, J., 1979. Hydraulics of Groundwater. McGraw Hill, New York.
Bouwer, H., 2002. Artificial recharge of groundwater: hydrogeology and engineering. Hydrogeology Journal 10, 121–142.
Buès, M.A., Oltean, C., 2000. Numerical simulations for saltwater intrusion by the mixed hybrid finite element method and discontinuous finite element method. Transport in Porous Media 40, 171–200.
Chang, S.W., Clement, T.P., 2012. Experimental and numerical investigation of saltwater intrusion dynamics in flux-controlled groundwater systems. Water Resources Research 48, W09527.
Chang, S.W., Clement, T.P., 2013. Laboratory and numerical investigation of transport processes occuring above and within a saltwater wedge. Journal of Contaminant Hydrology 147, 14–24.
Chang, S.W., Clement, T.P., Simpson, M.J., Lee, K.K., 2011. Does sea-level rise have an impact on saltwater intrusion? Advances in Water Resources 34, 1283–1291.
Chapra, S.C., Canale, R.P., 2009. Numerical methods for engineers, sixth ed. McGraw Hill, Singapore.
Clement, T.P., Wise, W.R., Molz, F.J., 1994. A physically based, two-dimensional, finite-difference algorithm for modeling variably saturated flow. Journal of Hydrology 161, 71–90.
Daher, W., Pistre, S., Kneppers, A., Bakalowicz, M., Najem, W., 2011. Karst and artificial recharge: theoretical and practical problems a preliminary approach to artificial recharge assessment. Journal of Hydrology 408, 189–202.
Ellery, A.J., Simpson, M.J., McCue, S.W., Baker, R.E., 2012a. Critical time scales for advection-diffusion-reaction processes. Physical Review E 85, 041135.
Ellery, A.J., Simpson, M.J., McCue, S.W., Baker, R.E., 2012b. Moments of action provide insight into critical times for advection-diffusion-reaction processes. Physical Review E 86, 031136.
Ellery, A.J., Simpson, M.J., McCue, S.W., 2013. Comment on local accumulation time for source, diffusion and degradation models in two and three dimensions. Journal of Chemical Physics 139, 017101.
Goswami, R.R., Clement, T.P., 2007. Laboratory-scale investigation of saltwater intrusion dynamics. Water Resources Research 43, W04418.
Grimmett, G., Welsh, D., 1986. Probability: An Introduction. Oxford University Press, Oxford.
Haitjema, H.M., 1995. Analytic element modeling of groundwater flow. Academic Press, San Diego, USA.
Hickson, R.I., Barry, S.I., Mercer, G.N., 2009a. Critical times in multilayer diffusion. Part 1: Exact solutions. International Journal of Heat and Mass Transfer 52, 5776–5783.
Hickson, R.I., Barry, S.I., Mercer, G.N., 2009b. Critical times in multilayer diffusion. Part 2: Approximate solutions. International Journal of Heat and Mass Transfer 52, 5784–5791.
Hickson, R.I., Barry, S.I., Sidhu, H.S., Mercer, G.N., 2011. Critical times in single-layer reaction diffusion. International Journal of Heat and Mass Transfer 54, 2642–2650.
Kim, D.J., Ann, M.J., 2001. Analytical solutions of water table variation in a horizontal unconfined aquifer: constant recharge and bounded by parallel streams. Hydrological Processes 15, 2691–2699.
Kreyszig, E., 2006. Advanced Engineering Mathematics. John Wiley and Sons.
Landman, K.A., McGuinness, M.J., 2000. Mean action time for diffusive processes. Journal of Applied Mathematics and Decison Sciences 4, 125–141.
Lu, C., Werner, A.D., 2013. Timescales of seawater intrusion and retreat. Advances in Water Resources 59, 39–51.
Martín-Rosales, W., Gisbert, J., Pulido-Bosch, A., Vallejos, A., Fernández-Cortés, A., 2007. Estimating groundwater recharge induced by engineering systems in a semiarid area (southeastern Spain). Environmental Geology 52, 985–995.
McNabb, A., 1993. Mean action times, time lags, and mean first passage times for some diffusion problems. Mathematical and Computer Modelling 18, 123–129.
McNabb, A., Wake, G.C., 1991. Heat conduction and finite measure for transition times between steady states. IMA Journal of Applied Mathematics 47, 193–206.
Pedretti, D., Barahona-Palomo, M., Bolster, D., Sanchez-Vila, X., Fernandez-Garcia, D., 2012. A quick and inexpensive method to quantify spatially variable infiltration capacity for artificial recharge ponds using photographic images. Journal of Hydrology, 118–126.
Remson, I., Hornberger, G.M., Molz, F.J., 1971. Numerical Methods in Subsurface Hydrology, with an Introduction to the Finite Element Method. Wiley Interscience, New York.
Simpson, M.J., Clement, T.P., Gallop, T.A., 2003. Laboratory and numerical investigation of flow and transport near a seepage-face boundary. Ground Water 41, 690–700.
Simpson, M.J., Ellery, A.J., McCue, S.W., Baker, R.E., 2013. Critical timescales and time intervals for coupled linear processes. ANZIAM Journal 54, 127–142.
Sophocleus, M., 2012. On understanding and predicting groundwater response time. Ground Water 50, 528–540.
Strack, O.D.L., 1989. Groundwater Mechanics. National Water Well Association, Ohio.
Vandenbohede, A., Van Houtte, E., 2012. Heat transport and temperature distribution during managed artificial recharge with surface ponds. Journal of Hydrology 472–473, 77–89.
Walton, W.C., 2011. Aquifer system response time and and groundwater supply management. Ground Water 49, 126–127.
Wang, H.F., Anderson, M.P., 1982. Introduction to groundwater modeling. Finite difference and finite element methods. Academic Press, California, USA.
Watson, T.A., Werner, A.D., Simmons, C.T., 2010. Transience of seawater intrusion in response to sea level rise. Water Resources Research 46, W12533.
Zheng, C., Bennett, G.D., 2002. Applied Contaminant Transport Modeling, second ed. John Wiley and sons, New York, USA.
Zill, D.G., Cullen, M.R., 1992. Advanced Engineering Mathematics. PWS Publishing Company, Boston, USA.